Available online at www.sciencedirect.com

ScienceDirect

journal homepage: http://www.elsevier.com/locate/acme

Original Research Article

Stress concentration factors of shear connection by composite dowels with MCL shape

M. Kożuch, W. Lorenc

Wrocław University of Technology, Wybrzeże Wyspiańskiego 27, 50-370 Wrocław, Poland

ARTICLE INFO

Article history:
Received 27 January 2017
Accepted 25 August 2018
Available online 22 September 2018

Keywords:
Composite dowel
Composite structure
Continuous shear connection
FE analysis
Laboratory test

ABSTRACT

In this paper, the authors present studies leading to the evaluation of the elastic resistance of the steel part of a continuous shear connection named MCL dowel. The MCL dowel is now the most commonly used shape of continuous connector, chosen among many others for its combination of good fatigue, elastic, and ultimate resistances. A method for the calculation of stress in the steel dowel is described in the paper. It is based on mathematical derivations followed by FE analysis. It is assumed that the steel connector is stressed as a result of a global stress state at the dowel root (being a part of the entire beam) and of a local effects of longitudinal shearing between the steel and concrete parts. Results of the mathematical derivations are confirmed experimentally. Full-scale tests of beam elements were performed with measures of strain in many points of selected connectors. A comparison of strains derived from the proposed design methodology and measured during the experimental tests is shown and discussed. The results herein presented are fundamental research which were one of backgrounds for fatigue limit states of composite dowels for purposes of implementation of composite dowels to the second version of Eurocode 1994-2.

1. Introduction

In the framework of the project *Precobeam* [1], a new method in steel-concrete composite beams was developed to connect a steel beam with a concrete slab using continuous shear connectors instead of widely used headed studs. These connectors were formed by cutting the web of an I-beam with specific line, so to obtain two T-beams which webs were terminated by connectors, see Figs. 1, 2 and 3.

After casting and hardening of concrete part of composite beam, the connectors embedded in the surrounding concrete guaranteed an effective transfer of the longitudinal shear forces between steel and concrete part of the beam. This was because of interlocking of concrete dowels between steel connectors. This way new, effective method of composition steel and concrete parts into one composite beam was developed. Contrary to headed studs, application of continuous shear connectors allowed for obtaining steel part of a composite beam in a fully automatic way. Advantage of composite beams with this type of connectors is also significant reduction of steel consumption, as in compressed parts of cross-section steel may be completely eliminated and replaced by much cheaper concrete.

During the realization of the project [1], several static and cycling tests have been carried out on elements (POST elements, newly designed NPOT elements and beams) with

E-mail address: maciej.kozuch@pwr.edu.pl.
https://doi.org/10.1016/j.acme.2018.08.006
1644-9665/

Nomenclature

MCL	modified clothoidal shape of the connector, considered in the paper (Fig. 4)
NPOT	new push-out test [1], modified version of POST, in which applied force generates tensile stress in the connector's base
FEM	finite element method
$\sigma_G(s)$	stresses at the dowel's edge caused by global effects (normal force and bending moment in the beam) at the s-coordinate point, including notch effect
s	local coordinate at the dowel's edge (Fig. 5)
σ_N	stress value at level of the base of the connector caused by global effects calculated by any means (e.g. with the well-known methods of theory of elasticity), without a notch effect (Fig. 5)
$A_G(s)$	function describing the change of σ_N stresses at the edge of the connector in correspondence of the coordinate s [1,15,21]
$\sigma_L(s)$	stresses (reduced or principal) at the dowel's edge caused by local effects (longitudinal shearing force acting on the connector) at the s-coordinate point, including notch effect
σ_{VL}	Stress value at level of the base of the connector caused by local effects calculated by any means (e.g. with the well-known methods of theory of elasticity), without a notch effect
$A_L(s)$	function describing the change of σ_{VL} stresses at the edge of the connector in correspondence of the coordinate s [1,15,21]
f	function describing resultant stresses at the edge of connector being the sum of $\sigma_G(s)$ and $\sigma_L(s)$ (which are defined above)
$\frac{1}{k_L}$ and $\frac{1}{k_{L,1}}$	stress concentration factor for stresses resulting from longitudinal shearing force, respectively for reduced and first principal stress
$\frac{1}{k_G}$ and $\frac{1}{k_{G,1}}$	stress concentration factor for stresses resulting from global effects, respectively for reduced and first principal stress

connectors having various shapes [1,2]. The strain on open connectors, which are an integral part of the web of the steel beam, depended not only on the longitudinal shearing forces, but also on the global distribution of normal stresses in the beam. Since bridge engineering was the main area of application of the solutions being considered, a lot of attention was paid to fatigue resistance and therefore also to the need to determine the state of stresses in the connector, so its elastic resistance. Problems with fatigue resistance had already been noticed in the framework of the Precobeam project [1]. When searching for the optimal shape of the connector (see also [3–5]), fatigue cracks propagating until total rupture of the steel beam were observed during the cyclic tests [1,6–9]. The optimal shape was supposed to combine a both high ultimate and fatigue resistance, high ductility and the simplicity of cutting the beam in order to manufacture it [10]. Finally, for the construction of a bridge, as shown in [11] a method was developed for cutting the web so that the continuous move of the cutter resulted in two identical T-beams with connectors based on a clothoidal line (see Figs. 1, 2 and 3). Extensive studies on this shape, considered optimum and from here on referred to as the MCL dowel (Fig. 4), were carried out after completion of the Precobeam project, in the framework of the ELEM project [12] – to determine the limit capacity, and [13,16] – elastic and fatigue capacity. The results of studies related to the ultimate capacity have been published, among others, in [13,14,17]. The rest of this article focuses on identifying the elastic capacity of the MCL dowel.

2. General idea of elastic resistance evaluation

Continuous connectors that are part of a steel beam (and of the composite one) cannot be treated the same way as discrete connectors (for ex. headed studs). That is because the stress distribution within the connector is not only the result of the longitudinal shear forces acting on it (named hereafter as local effects), but also of the stress associated with the global internal forces in the steel beam: bending moment and axial force, named hereafter as global effects. The concept of elastic capacity developed by Lorenc [15] assumes a linear summation of the above mentioned effects in each point of the connector's edge. [21] is summary of [15] in English. Therefore, to determine the resultant distribution of stresses on the edge of the connector, it is first necessary to determine the distribution of stresses on its edge, deriving from both the longitudinal shear force acting on the connector (local effects) and the normal stresses present at the base of the connector and linked to the global bending moments and axial forces in the beam (global effects). The determination of the normal stresses caused by global effects at the base of the connector is relatively simple. Stress state depends only on the geometry of the connector, which is treated as a notch geometry, increasing the normal stresses at its base. It is then assumed

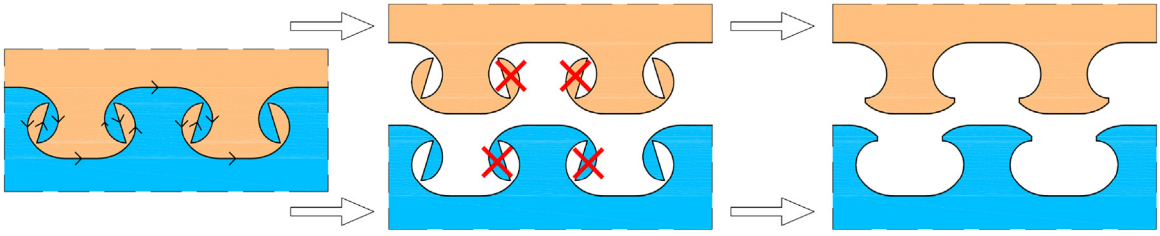

Fig. 1 – General idea of cutting an I-beam so to obtain steel continuous shear connectors (on example of MCL shape).

Fig. 2 – Consecutive stages of obtaining steel T-beams with MCL connectors.

Fig. 3 – Steel beams with continuous shear connectors before application in animal crossing bridge PE4 over S7 expressway in Poland.

that the value of appropriate type of stress (reduced or principal) in any point on the edge of the connector will be:

$$\sigma_G(s) = \sigma_N \cdot A_G(s) \tag{1}$$

where all symbols are explained in the list of symbols at the beginning of the paper (see also Fig. 5).

It is more complicated to determine the stress distribution in the connector resulting from the action of the longitudinal shear force (local effect). That is because such distribution depends on the geometry of the connector as well as the interrelation between the stiffness of the steel and concrete parts, and on the frictional forces between steel and concrete, which are always present on the faces of the connector. Even by assuming the elastic parameters of both steel and concrete, the calculation becomes non-linear due to contact issues. FEM is an effective method to determine this distribution. The variability of stresses on the edge of connector can be presented using the formula below, where depending on the needs, either the equivalent stresses according to the Huber-Mises hypothesis (elastic capacity) or the principal stress (the stress variation for fatigue analysis) are taken into account:

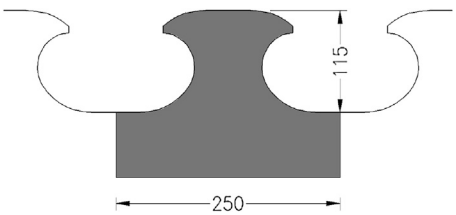

Fig. 4 – General geometry of MCL shear dowel.

$$\sigma_L(s) = \sigma_{VL} \cdot A_L(s) \tag{2}$$

where all symbols are explained in the list of symbols at the beginning of the paper.

Assumptions adopted in the analysis:

1 the value of stress σ_N and σ_{VL} at a level of the dowel's base can be calculated by any means, e.g. with the well-known methods of the theory of elasticity, in which cross-sectionals parameters (an area, a moment of inertia, a location of neutral axis) can be calculated using the modular ratio method – assuming a substitute homogenous section, which takes into account different elastic constants of steel and concrete part of the section – as described e.g. in EN 1994-1-1,
2 approach for the stress evaluation in the steel dowel is presented hereafter as the answer of the connector to applied forces. The influence of the stiffness of the dowel on the distribution of longitudinal shearing force acting on the connector as well as on the normal stress distribution in the cross section of the beam is not the aim of the paper. Thus the slip between steel and concrete and its influence on global internal forces in the beam is not discussed. The stiffness of 1 m of the considered connection is comparable to connections with headed studs applied [17] and calculation of internal forces in the beam can be made with similar methods. Interlayer slip is taken into account on the local level for determination of stresses in the connector caused by already known shearing force,
3 the final stress state at the edge of the connector is calculated as linear summation of stresses resulting from local and global effects. This is accurate approach for the principal stresses and safe-sided approximation for the reduced stresses (see also extra explanations in Section 5).

Having defined the functions describing the distribution of reduced (or principal) stresses on the edge of the connector, the elastic capacity can be determined through the following steps [15]:

- evaluation of the function $f(s)$, defined as the sum of the global and local effects (Eq. 3),
- differentiation of function $f(s)$ and determination of the zeros of the derivative, in order to determine the point s of maximum stresses at the edge of the connector i.e. s* (Eq. 4),
- calculation of the maximum value of f-function $\max(f(s)) = f(s*)$. It defines the maximum stress value at

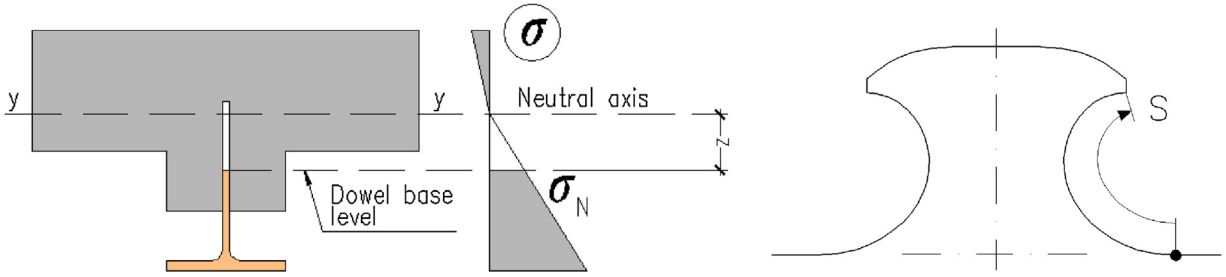

Fig. 5 – Elastic stress at dowel base level calculated without notch effect (left side) and s-coordinate (right side).

the edge of the connector, taking into account notch effect. The maximum stress should be limited to e.g. yield strength of the steel (Eq. 5).

$$f(s) = A_{G,i}(s) \cdot \sigma_N + A_{L,i}(s) \cdot \sigma_{VL} \tag{3}$$

where:
i = M (reduced stresses) or G (principal stresses),

$$\frac{df(s)}{ds} = 0 \quad \text{leads to} \quad s* \tag{4}$$

$$f(s*) = \max(f(s)) \leq f_y \tag{5}$$

The result of the analysis carried out can be presented graphically as an interactive envelope of the steel connector's strength, in which the horizontal axis represents the dimensionless utilization ratio of the connector due to global effects (axial force and bending moment in the beam), and the vertical axis represents the dimensionless utilization ratio of the connector from the local effect (the transmission of longitudinal shearing forces between steel and concrete). Both utilization ratios already take into account the stress concentration resulting from the geometry of the steel connector. The idea of the envelope is shown in the following sketch (Fig. 6).

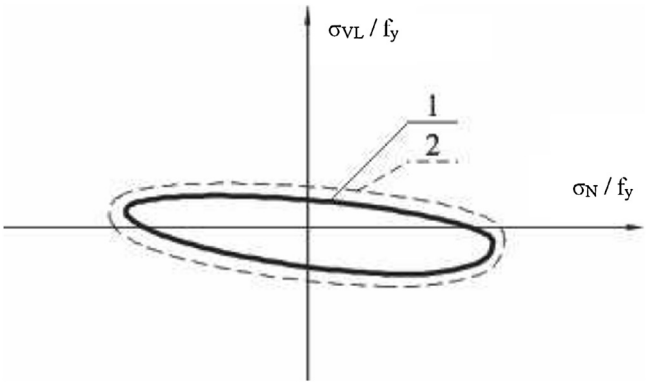

Fig. 6 – Envelope of the dimensionless elastic resistance. 1 and 2 stand for different possible connector shapes [15].

3. FE analysis

In order to properly define the $A_G(s)$ and $A_L(s)$ functions describing the stress distribution at the edge of the connector, fragmentary FE models have been prepared using the *ABAQUS* 6.10 software [18], each for a separate analysis of the global and local effects. Based on preliminary parametric analyses, the size of the finite element in the field of the connector's base has been set to 1 mm; the element type C3D8R (continuum three-dimensional of 8 nodes element with reduced integration) has been used with only 1 element throughout the thickness of the connector; linearly elastic characteristics for both concrete (E_{cm} = 37 GPa) and steel (E_{and} = 210 GPa) have been employed; the *hard contact* with the *small sliding formulation* approach has been used for the definition of contact issues; and the friction coefficient between steel and concrete, present only on the faces of the connector, has been considered equal to 0.3. Nonlinear characteristics of concrete have not been introduced into the analysis, in which the objective was to determine the elastic capacity of the steel connector, due to the negligible impact on the results [1,19]. The influence of defining the contact issue through the *small* rather than *finite sliding formulation* was determined to be lower than 1%, because the elastic capacity of the connector is achieved with slides several times smaller than the accepted size of the finite element mesh. The impact on the results obtained of variations of Young's modulus for steel, in the range of 200–210 GPa, was 0.5%, whereas changes in the modulus of elasticity of concrete in the range 32–41 GPa led to a difference in results of approx. 5% (thus the analysis was carried out with the average modulus value of 37 GPa). The coefficient of friction on the faces of the connector has the greatest impact on the stress distribution obtained on its edge. The preliminary parametric analysis covered friction coefficients in the range of 0–0.5 and, for these limits, a greater friction coefficient resulted in lower values of the maximum stress, but also a different point at the edge of the connector where maximum stress appears (differences of approx. 12%). Due to the fact that the pressure stresses always occur on the faces of the connector, an average value of friction coefficient of 0.3, considered as a safe estimate, has been accepted for further analysis.

A model (Fig. 7), used to determine the impact of the notch geometry on the increase in global stresses at the base of the connector, was a simple plate with geometry of the MCL connectors. The model was subjected to the action of uniform normal stresses (L1) in the direction of the Z axis and applied to one of the side faces of the plate. On the opposite surface, the

slide capacities were blocked (BC3: uX = uY = uZ = 0), the boundary condition imposed on the entire bottom surface of the plate was in the form of a slide support (BC2: uY = 0), whereas symmetry planar conditions (BC1: uX = urY = urZ = 0) were imposed on the lateral surface. In the description of the boundary conditions, "u" refers to a slide along the predetermined axis, while "ur" indicates the rotation condition relative to the reference axis.

The normal stresses (L1) applied in the A model, equal to 50 MPa (treated as a unit load), result in stresses in the vicinity of the connector, shown in Fig. 8, and in the stress distribution along the edge of the connector, as in Fig. 9.

In actual constructions, the boundary conditions of the connector's work can be slightly different because, depending on the stress distribution in the composite beam, the connectors in the compressed concrete can be locked in the longitudinal direction. For this reason, additional analysis of comparative models have been performed, in which contact between the connector and the surrounding concrete is defined, and the stress was modeled to reflect the possible distributions of global stresses in the beam. Four models were considered (see Fig. 10). The basic model A without surrounding concrete and pure tension (GLOB-0) and three models with surrounding concrete and different stress distribution were analyzed: under uniform tension (GLOB-1), under tension with bending resulting in zero strain at concrete top fibers (GLOB-2) and under pure bending (GLOB-3). The results of the analysis are shown in Fig. 10.

It is visible, that limiting the free deformation of the upper part of the connector in the surrounding concrete has a positive effect on its strain, reducing the stresses by up to approx. 9% (for studied cases). To determine the elastic capacity of the connector, while excluding from the analysis the variable representing normal stress distribution at the height of the beam, it was decided to use the A model without a concrete slab. This assumption is treated as a safe sided simplification leading to upper estimation on stress along the connector's edge. The function $A_G(s)$, calculated as a reduction of A_{FEM} function presented in Fig. 9 to a unit load, will therefore have the form (Eq. 6):

$$A_{FEM}(s) = -0.0245 \cdot s^2 + 0.38 \cdot s + 74$$

$$k_{G,0} = \frac{1}{\sigma_{FEM}} = \frac{1}{50} = 0.02 \tag{6}$$

$$A_G(s) = k_{G,0} \cdot A_{FEM}(s) = -0.00049 \cdot s^2 + 0.0076 \cdot s + 1.48$$

where:
σ_{FEM} – normal stress applied in the A model (50 MPa)

To determine the influence of a local pressure of concrete on the face of the steel connector (and therefore the effect of the longitudinal shear between steel and concrete) on the state of stresses in the same connector, the B model was used. The geometry corresponds to the cut out part of the entire composite beam and was constructed by the plate represented in the A model, stiffened at the base through a horizontally placed steel plate (a flange corresponding to those present in real I-beams) and connected to the concrete slab with one connector (Fig. 11). The load in the considered model consists of the concentrated force applied to the concrete block (L2). Similarly to the A model, the BC1, BC2 and BC3 boundary conditions have been applied. In addition, a rigid connection between all nodes located on the end faces of the concrete block was introduced, together with limitation of rotation of these faces (BC4: urX = urY = 0). This prevent the rotation of the concrete slab against the steel beam and thus ensures that the planar cross-section before loading will remain the same after the load is applied. On the front and end faces of the center steel connector, marked

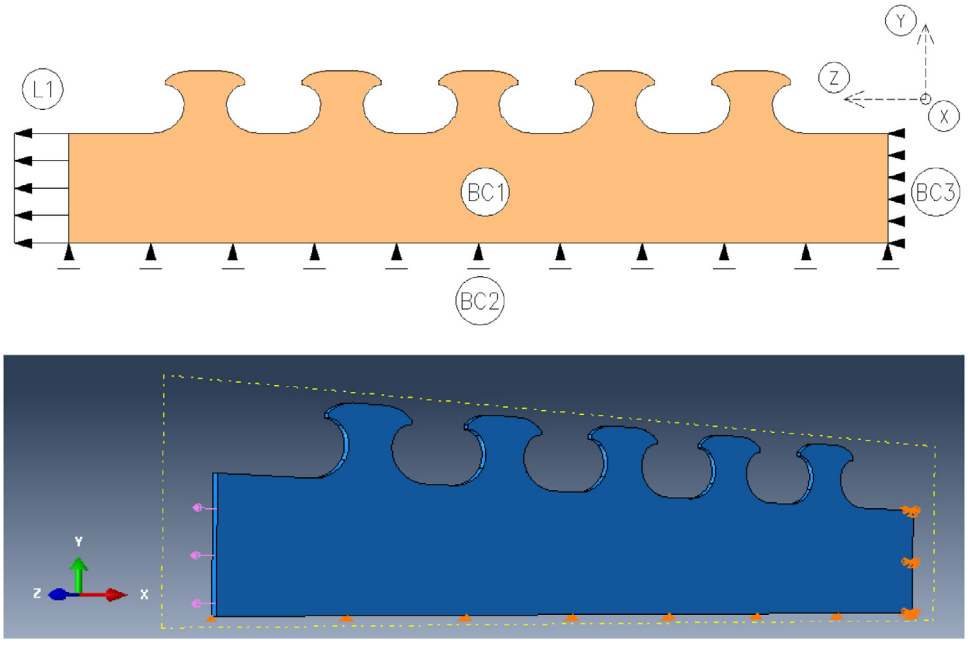

Fig. 7 – Model A – evaluation of influence of global effects on stress layout at the steel dowel's edge.

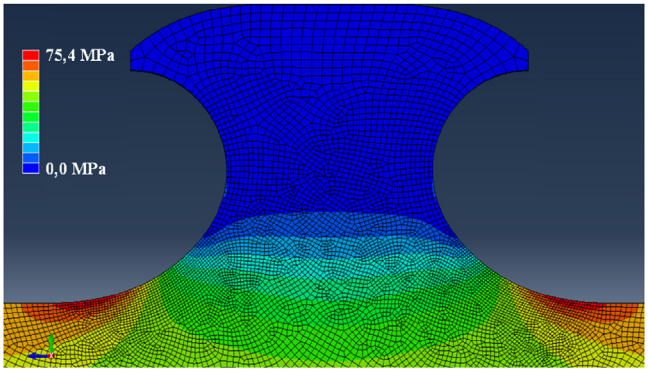

Fig. 8 – Stress plot in steel dowel – model A.

with (CON) in Fig. 11, a contact issue was introduced between steel and concrete, with the possibility of separating the two joined parts. A penetration of steel and concrete was prevented (*hard contact* [18]) and tangentially to the surfaces a friction contact with a coefficient of $\mu = 0{,}3$ (friction of steel on concrete) was defined. The impact of the height of the steel web and the size of the steel flange on the results obtained was the subject of a dissertation [15] and was proved to be low when the height of the webs is comparable to the length of the connector; hence, in the model adopted here, cross-sectional dimensions corresponding to the tested beams was considered (see Fig. 16a). The analysis of the B model is non-linear due to the contact issue; however, the linear material laws have been applied. The proposed model is a simplification of the issue, because it does not take into account the effect of the vertical shear forces on the stress values at the edge of a connector. The general model that takes into account this impact is presented in [17], where broad convergence of results obtained with both models has been demonstrated.

The force (L2) applied in the B model, reflecting the longitudinal shear force amounting to 25 kN (treated as a unit load), with the spacing of connectors of 250 mm and the modeled thickness of the web (5.2 mm – as half the thickness of the IPE500 web, what corresponds to dimensions used during laboratory tests) results in stresses in the vicinity of the connector, shown on Fig. 12, and in the stress distribution along the edge of the connector as in Fig. 13. The subscript T and C in the description of approximating polynomials A_{FEM} in the Fig. 13 means, that the analysis concerns the stress distribution on the side of the connector of the B model, where longitudinal shear force causes tensile (T) or compression (C) stresses, respectively. Subscripts MISES and PRINC denote reduced Huber-Mises and principal stresses respectively.

The $A_{L,\dots}(s)$ functions, calculated as a reduction of $A_{FEM,\dots}$ functions presented in Fig. 13 to a unit load, is used to analyze the stresses reduced with the Huber-Mises hypothesis and the principal stresses. It will have the form shown in Fig. 13, multiplied by a factor (Eq. 7):

$$k_{L,0} = \frac{e \cdot t_{FEM}}{P_{FEM}} = \frac{0.25 \times 0.0051}{0.025} = 0.051 \qquad ((7))$$

The final forms of the $A_{L,\dots}(s)$ functions are shown below (Eq. 8):

$$\begin{aligned} A_{L,MISES,T}(s) &= k_{L,0} \cdot A_{FEM,MISES,T}(s) \\ &= -0.00166 \cdot s^2 + 0.1805 \cdot s + 3.009 \end{aligned}$$

$$\begin{aligned} A_{L,PRINC,T}(s) &= k_{L,0} \cdot A_{FEM,PRINC,T}(s) \\ &= -0.00215 \cdot s^2 + 0.1668 \cdot s + 3.213 \end{aligned} \qquad (8)$$

$$\begin{aligned} A_{L,MISES,C}(s) &= k_{L,0} \cdot A_{FEM,MISES,C}(s) \\ &= -0,00144 \cdot s^2 + 0,1326 \cdot s + 1,530 \end{aligned}$$

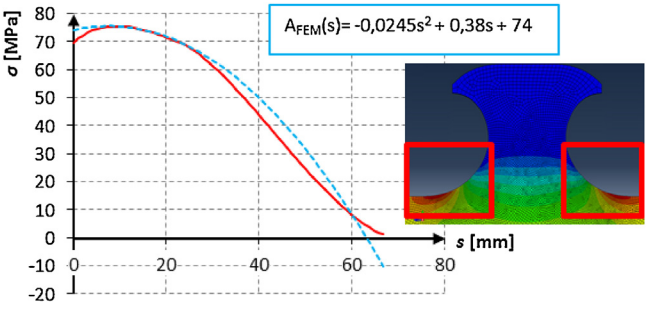

Fig. 9 – Stress values at the dowel edge and its approximation with 2nd order polynomial (A_{FEM}).

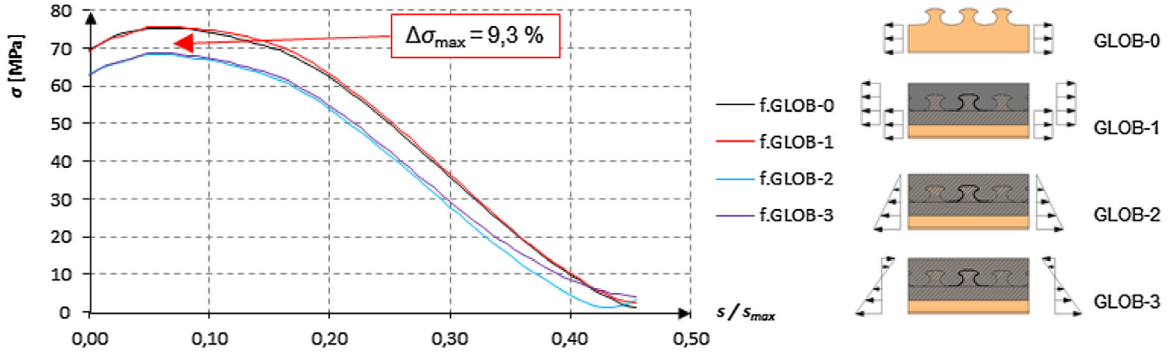

Fig. 10 – Influence of global stress state in the beam on the stress layout in the dowel's edge.

$$A_{L,PRINC,C}(s) = k_{L,0} \cdot A_{FEM,PRINC,C}(s)$$
$$= 0.001326 \cdot s^2 - 0.1275 \cdot s - 1.530$$

4. Elastic resistance of MCL steel dowel

Having defined the $A_G(s)$ and $A_L(s)$ functions, the elastic stresses can be determined at any point s along the connector's edge for any combination of the M, N, and V internal forces in the considered cross section of the composite beam, or the interactive envelope of the connector's load capacity, as shown in Section 2 (Eqs. (1) and (2)), can be determined. The above described approach developed to determine the envelope of the load capacity can be used in cases where the signs of stresses deriving from the local and global effects are the same. This is because the summation of two convex functions, with extremes in the considered s area, will also result in a convex function having extremes in the considered range, regardless of the numerical values of σ_N and v_L. For all other cases, instead of an analytical approach, the numerical approach can be applied. Assuming a fixed stress value for one of the effects (global or local), the stress deriving from the second effect is evaluated so that, at the edge of the connector, the yield strength is reached. For principal stresses, the presented approach, including summation of stresses from the global and local effects, is accurate; for reduced stresses it is only an approximation, but safe-sided. This is because the values of reduced stresses from both models, rather than their components, are added. Therefore, the received envelopes of load capacity have the correct values at the intersection of the axis, but their process is somewhat ``flattened''. This approach guarantees safety, does not generate a large error, and greatly simplifies the analysis.

The envelope of the connector's load capacity for reduced stresses according to the Huber-Mises hypothesis, used to check the elastic resistance, is shown in Fig. 14. The main stress is depicted in Fig. 15. Each quadrant of the chart describes the situations deriving from different combinations of signs of stresses, attributable to global and local effects in the area of connector under consideration (as shown schematically in the diagrams in each quadrant of the graph). For example, in the I quadrant, tensile stresses from the global effects, and tensile stresses from the local effects, are summed; in the II quadrant, tensile stresses from the global effects, and the compressive stresses from the local effects are summed, etc.

The fields marked in red were not analyzed in detail, because they will never be decisive in reaching the elastic resistance of the connector. Stresses from the global and local effects are opposite in sign, and thus the elastic resistance of the connector will certainly be reached in conditions described by the area on the opposite side (in the next quadrant of the graph).

In the above analysis, the edge's length $0 \le s \le 63$ mm was considered, where the 0 point was adopted as shown in Fig. 5 (the beginning of the fillet at the base of the connector).

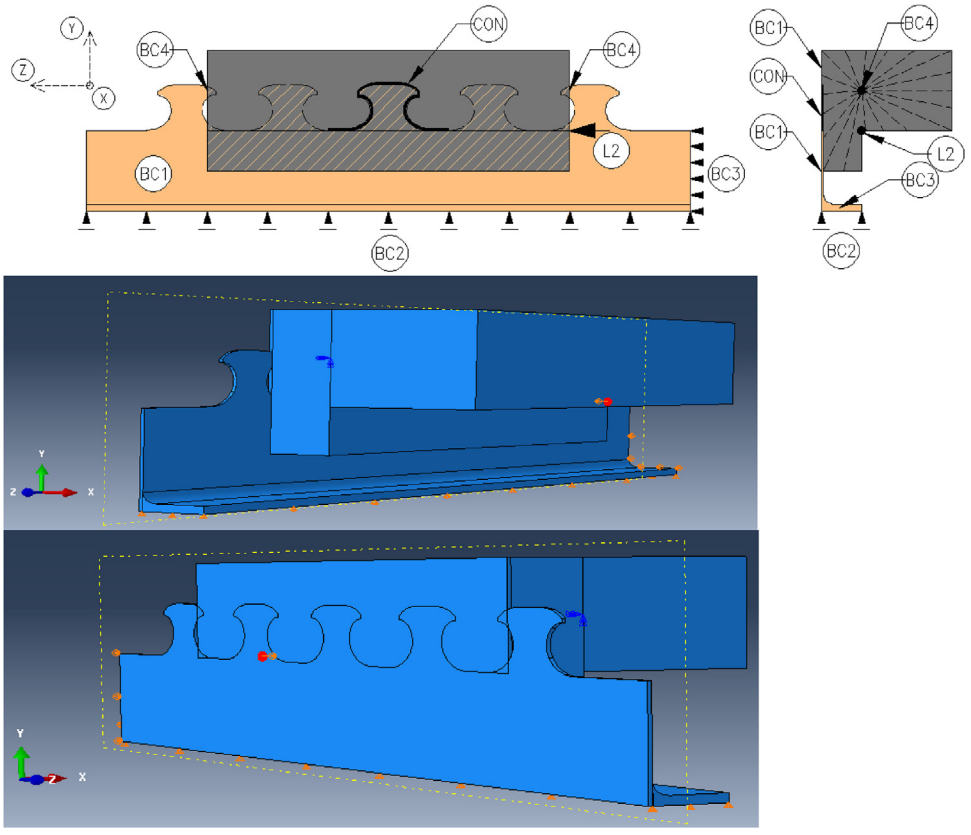

Fig. 11 – Model B – evaluation of influence of local effects on stress layout at the steel dowel's edge.

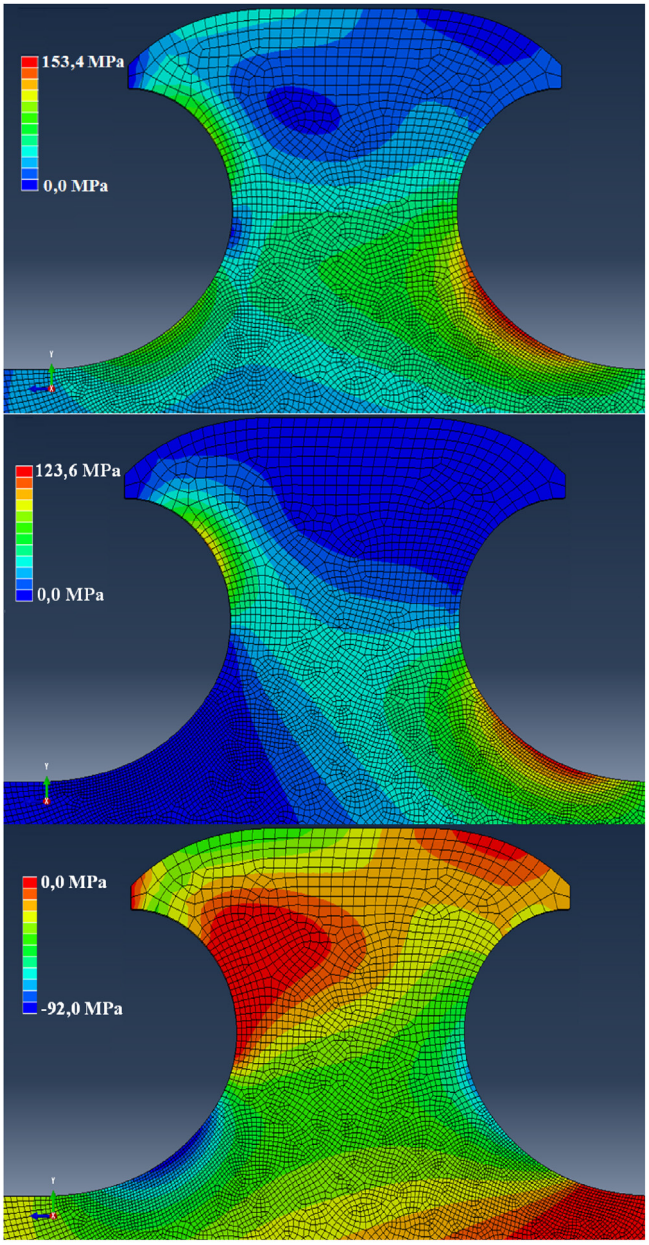

Fig. 12 – Stress plots in steel dowel – model B. Top: Mises stress, middle: max. principal stress (tensile), bottom: min. principal stress (compressive).

The variability of stresses on this length, considered decisive for the load capacity of the connector, was described by mathematical functions. The dotted lines in the above envelope mark sections for which the yield strength was obtained at the edge of the analyzed area ($s = 0$ or $s = 63$ mm). When both the normal stress acting on the beam and the stresses caused by longitudinal shear force have opposite sings (quadrants II and IV), simultaneous increasing both of them may lead to the attainment of the elastic capacity of the element in points located outside the analyzed section. The envelopes presented in the areas marked with dotted lines relate to precisely such a situation, they should be treated demonstratively, bearing in mind the possibility of early destruction of the element in the areas not considered in the analysis; however, these are purely hypothetical situations, since in such cases the destruction of the connector will always be described by curves in quadrants I or III.

Based on the above analysis, the elastic resistance of the connector can be described analytically:

- in the serviceability limit state (elastic resistance) (Eq. 9):

$$\sigma_s = \sigma_L + \sigma_G \leq f_y \tag{9}$$

$$\sigma_L \leq f_y$$

$$\sigma_G \leq f_y$$

$$\sigma_L = \frac{1}{k_L} \cdot \sigma_{VL}$$

$$\sigma_G = \frac{1}{k_G} \cdot \sigma_N$$

$$k_G = 0,663$$

$$k_L = \begin{cases} 0,126 - \text{while analyzing the tension zone of the connector} \\ 0,218 - \text{while analyzing the compression zone of the connector} \end{cases}$$

in the fatigue limit state (Eq. 10):

$$\Delta\sigma_s = \Delta\sigma_L + \Delta\sigma_G \leq \Delta\sigma_C/\gamma_{Mf} \tag{10}$$

$$\Delta\sigma_L = \frac{1}{k_{L,1}} \cdot \Delta\sigma_{VL}$$

$$\Delta\sigma_G = \frac{1}{k_{G,1}} \cdot \Delta\sigma_N$$

$$k_{G,1} = 0,663$$

$$k_{L,1} = \begin{cases} 0,155 - \text{while analyzing the tension zone of the connector} \\ 0,218 - \text{while analyzing the compression zone of the connector} \end{cases}$$

If gas cutting was adopted during beam manufacturing (in order to cut I-beam into two T-beams with continuous connectors), it is recommended to assume the fatigue category equal to 125 MPa and a partial factor for the fatigue limit consistent with Eurocode 3, depending on the adopted method of assessing fatigue life and the consequences of the destruction.

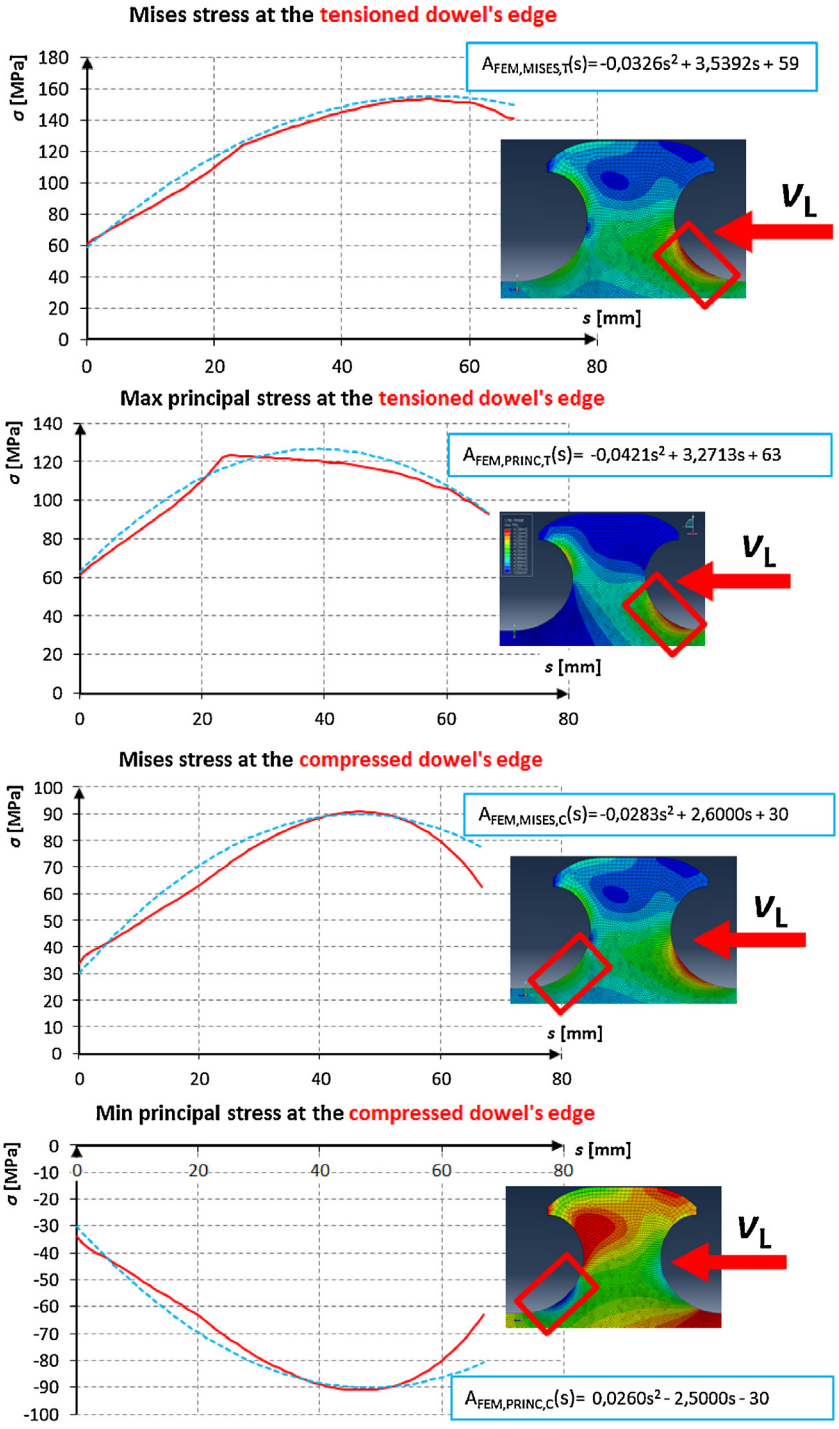

Fig. 13 – Stress (reduced Huber-Mises and max./min. principal) values at the dowel edges and approximation with 2nd order polynomials ($A_{FEM,\ldots}$).

5. Laboratory tests – setup

Three composite beams of natural scale, with MCL composite dowels, have been designed, manufactured and tested. For each of them, strain gauges have been placed in 10 points on the chosen connectors, allowing the evaluation of the convergence between the measures and calculated strains as the sum of strains obtained from the numerical models A and B. In this way, the proposed procedure for determining the load capacity of the connector has been indirectly verified by determining the convergence of the experimental and numerical results (the last are the basis for determining the

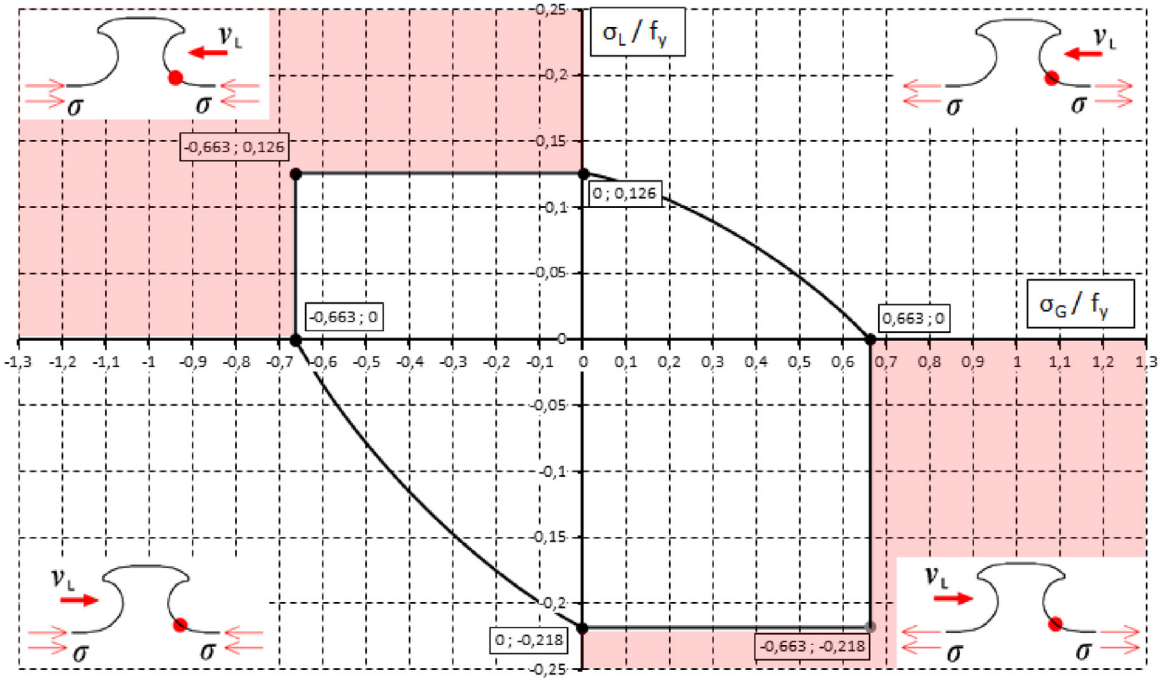

Fig. 14 – Envelope of elastic resistance of MCL steel dowel for Mises stress.

load capacity of connectors). Cross-sections of the tested beams are shown in Fig. 16, and a static scheme is reported in Fig. 19. Tested beams have been designed in such a way that in one of them the connectors level is close to the neutral axis of the beam thus the impact of global effects on a stress state in connectors is very small (beam B1), and for the other beam, the base of the connector is deep in its tension zone, resulting in considerable stress at the base of the connector from the global bending of the beam (beam B2). The tests involved two B1 beams and one B2 beam.

Connectors in the vicinity of the point in which loads were applied (on the support and under the concentrated

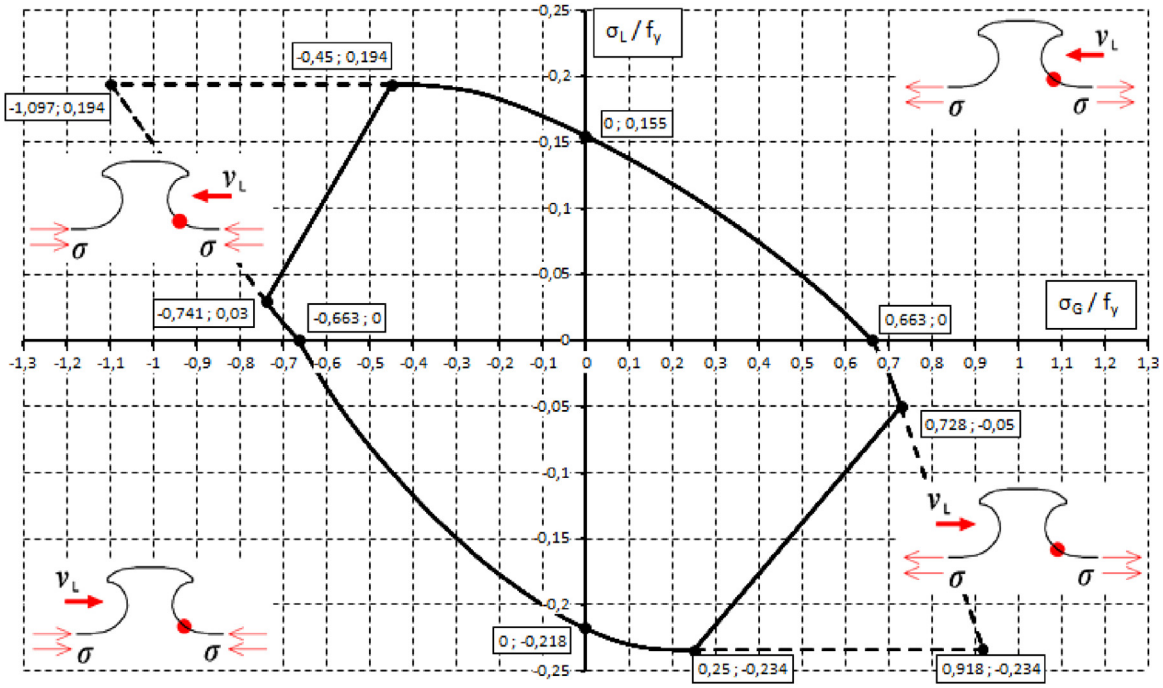

Fig. 15 – Envelope of elastic resistance of MCL steel dowel for first principal stress.

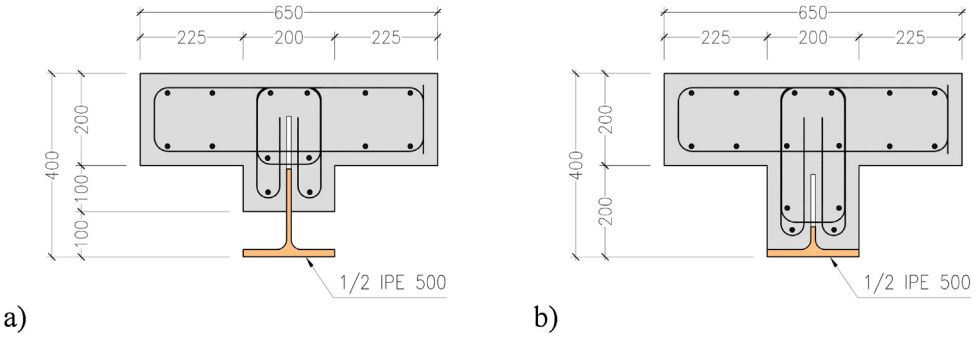

Fig. 16 – Cross sections of the beams subjected to laboratory tests. (a) beam B1, (b) beam B2.

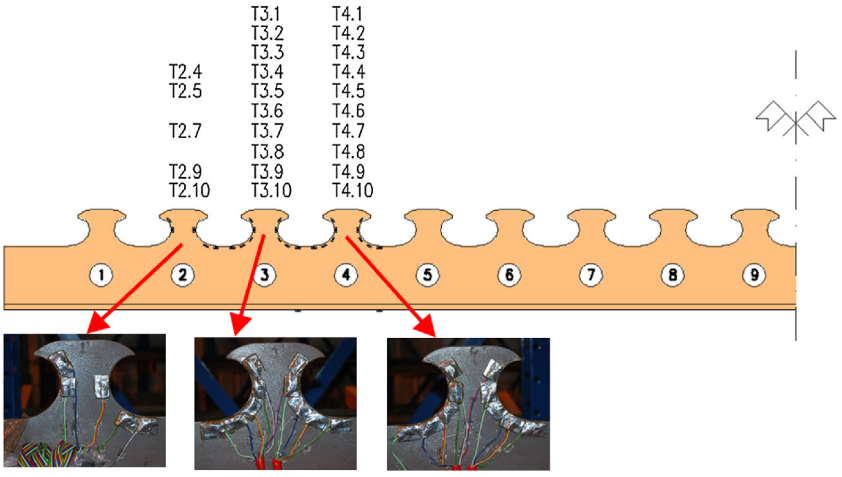

Fig. 17 – Strain gauges at steel dowels placed at the single beam.

forces induced by the testing machine) were clad in foamed polystyrene, to eliminate them from participating in the transmission of the longitudinal shearing forces, thereby eliminating local perturbations that would affect the value of the longitudinal shearing forces on the remaining connectors. The steel part of the beams was obtained by the longitudinal cut of the IPE500 profile from S355J2 steel (in Fig. 2) with an average yield strength obtained from the tensile tests of 443 MPa and with an ultimate tensile strength of 546 MPa, the concrete part was made of C50/60 concrete (with an average compressive strength of 74.2 MPa, determined in standard compressive tests at 150 × 150 × 150 mm cubes performed on the day of the beams tests) and the B500SP reinforcing steel.

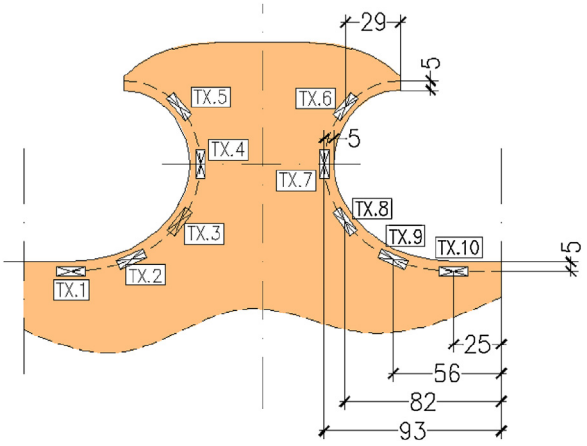

Fig. 18 – Exact localization of strain gauges at the single dowel.

The arrangement of strain gauges on the beam connectors is shown in Figs. 17 and 18, where the symbol TX.*n* denotes the strain gauge, *T*, at dowel no. *X* and place no. *n*.

The procedure adopted in loading the beams consisted first in the execution of 25 cycles of load within the range of 5–40% of the estimated beam's load capacity and then in the application of a static load until failure was reached. Strain measurements concerned the connectors, the lower flange of the steel beam, the upper and lower surfaces of the concrete slab, and the reinforcement bars. The measurement also covered deflections in 5 points on the beam length (sensors numbered 1–5), slip between the concrete slab and the steel beam (sensors no. 7, 8, 10, 11), as well as the uplift

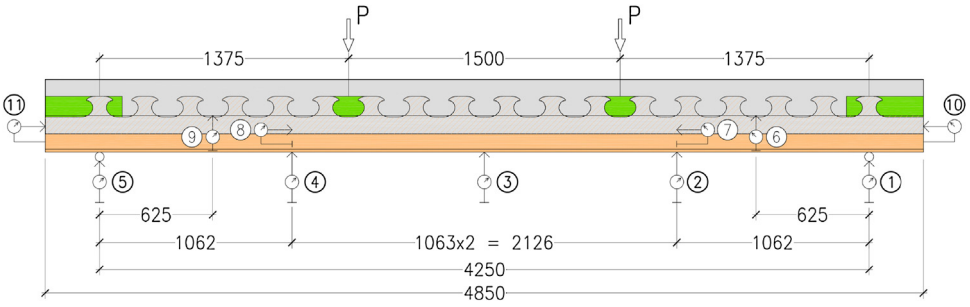

Fig. 19 – General view on static system for 4-point bending tests and arrangement of LVTD sensors.

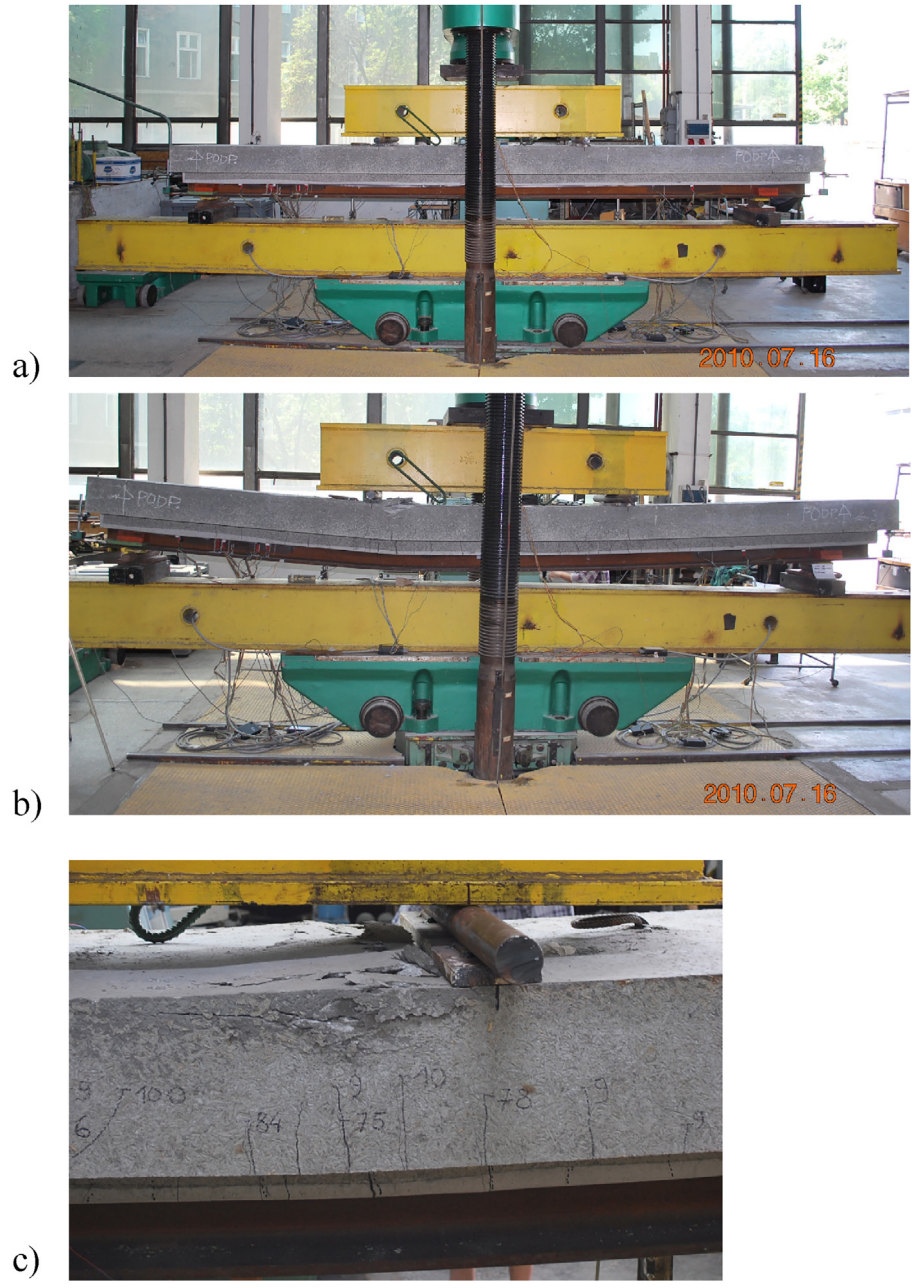

Fig. 20 – General view on B1 beam before (a) and after (b) tests and (c) arrangement of cracks in concrete slab. Cracking in compressive zone is visible.

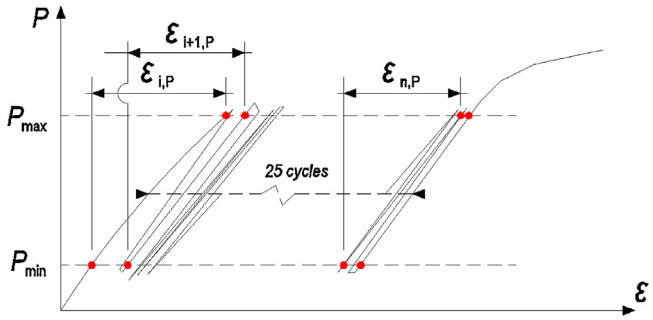

Fig. 21 – P–ϵ chart as a determination of $\epsilon_{i,P}$ values for FEA verification.

(no. 6 and 9). The schematic layout of inductive sensors is shown in Fig. 17.

6. Laboratory tests – results and discussion

Fig. 20 shows the selected beam (beam B1) before and after the tests carried out. All the beams underwent failure in the same way. At a certain load level (approx. 65% of ultimate load), an increase in slip between the steel and concrete could be observed. At the same time, transverse cracks began to develop in the lower fibers of the concrete slab. As the load reached approx. 80% of the ultimate load, the nonlinear increase in strain was observed in the lower flange of the beam, resulting in a significant increase of the deflection of the beam. The slippage between steel and concrete was growing much faster than in the initial phase and the transverse cracks in the concrete slab significantly increased both their width and range. When the ultimate load was approached, cracks with range indicating the lack of cooperation between steel and concrete could be observed in the concrete section. Beams were destroyed by brittle fracture of the reinforced concrete slab at the top, resulting from exceeding the limit strains in the compressed concrete.

In order to verify the proposed numerical models, only the elastic range of loading were analyzed. Readings for each strain gauge, located on steel dowels, were used for this purpose, with the strength close to the minimum, P_{min}, and maximum, P_{max}, values adopted during the first 25 loading cycles for each beam. In this manner, for each of the strain gauges, the readings of minimum and maximum strain, $\epsilon_{i,min}$ and $\epsilon_{i,max}$, were obtained, based on which the value of $\epsilon_{i,P}$, corresponding to the elastic deformation obtained with a force P equal to the difference between P_{max} and P_{min}, could be determined (Fig. 21).

After having obtained the 25 values of $\epsilon_{i,P}$, the extreme values were rejected, assuming, however, that the variability of the rest could be described with the t-Student distribution. Subsequently, the estimator of the standard deviation of the remaining trials was calculated, rejecting the 5% quantile with both-sided critical region. For the selected beam B1 connector, the convergence of numerical results (gray bars) with experimental results is shown in Fig. 22. The horizontal red and vertical black lines define the average value and the dispersion obtained in the laboratory strain readings, respectively. The comparison of strain for all 10 gauges placed close to the edge, on the front and rear faces of the single connector, was presented. Schematically, the location of the analyzed point is shown also in Fig. 22 (see also Fig. 18 with exact location of strain gauges). All experimental data is presented in [13], but for all analyzed connectors the convergence between numerically calculated and experimentally measured strains is very similar to this presented in Fig. 22.

It is noted that the variation of stresses in the vicinity of the circumferential line of the connector is large and the shift of the analyzed point by 1 mm may cause results to include a 10% deviation from the expected. Given the 3 mm length of the LY 11-3/120 strain gauge's measurement base and the precision of its application, exactly such inaccura-

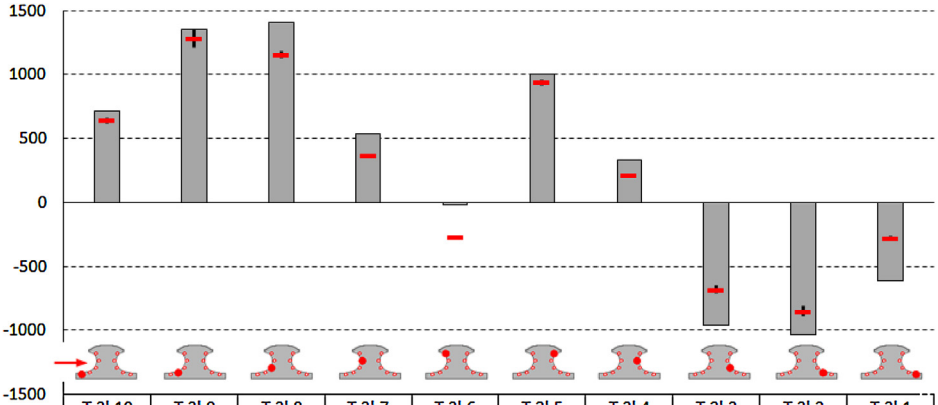

	T.3'.10	T.3'.9	T.3'.8	T.3'.7	T.3'.6	T.3'.5	T.3'.4	T.3'.3	T.3'.2	T.3'.1
εs,MES	719	1353	1407	539	-20	1002	331	-965	-1036	-614
εsMAX,P	664	1353	1184	380	-258	963	224	-648	-810	-257
εsMIN,P	617	1213	1128	351	-284	913	199	-714	-891	-296
εsŚR,P	643	1283	1156	368	-271	943	212	-681	-857	-279

Fig. 22 – Comparison of strains in steel dowel obtained from FEA and experimental test (description in text).

cies could have been expected. In addition, what authors underline, the model was not calibrated by changing the input parameters, including, in particular, the modules of elasticity of steel and concrete and the coefficient of friction. It is possible to assume such values of these parameters so to obtain almost exact convergence of experimental and numerical results. But such an approach has not been applied because these parameters will always take on a bit different values in actual structures. Their impact on the results is presented in section 3, and, to compare the experimental and numerical results, average values were adopted in the FEM model (as in sect. 3). However, it can be seen that the experimental and numerical results are in line, and the strains obtained numerically are slightly larger than those measured experimentally. Therefore, they constitute a secure foundation for the development of stress concentration factors from global and local effects, the values of which are of key importance in the procedure of determination of the elastic resistance of the steel connector, which is described in section 4.

7. Conclusions

On the basis of numerical analysis and experimental tests of composite beams with MCL dowels, it can be stated that:

- the FE numerical analysis of the steel part of open connectors can be used effectively to determine their elastic capacity,
- it is possible to determine the state of stress in the connector for any combination of internal forces acting on the composite beam, based on the combination of results of two fragmentary FE models. One is used to determine the notch coefficient, k_G, for global effects (bending moment and axial force in the beam), which results from the change in geometry of the T-beam web at the connector base; the second specifies the distribution of stresses in the connector due to the action of longitudinal shear force – stress concentration factor, k_L. The combined results from the two models were compared with the results of tests conducted on real beams. The good convergence of numerical and experimental results were obtained,
- knowing the above mentioned stress concentration factors for the global effects, k_G, and the local effects, k_L, it is not necessary to model the connector each time, and the maximum stresses in the connector are determined on the basis of the known internal forces in the beam and the geometric characteristics of the beam's cross-section. The load capacity of the connector can also be checked using the prepared connector capacity envelope,
- stresses in the connector for SLS (serviceability limit state) and FLS (fatigue limit state) analysis are defined as reduced and main principal, respectively. This results in other stress concentration factors, k_L. Determining the maximum permissible stresses in the connector in the SLS is an individual issue (it can be for example assumed, that they should not exceed the f_y or $1{,}3\,f_y$ yield strength of steel [20]). The amplitude of principal stresses for fatigue loads in the FLS should not exceed $\Delta\sigma_c$, which, in turn, depends on the manufacturing technology of the connectors (for ex. 125 MPa for automatic gas cutting).

Ethical statement

Authors state that the research was conducted according to ethical standards.

REFERENCES

[1] Preco-Beam, Prefabricated enduring composite beams based on innovative shear transmission RFSR-CT-2006-00030, final report, Project carried out with the financial grant of the Research Programme of the Research Fund for Coal and Steel (2009).

[2] W. Lorenc, E. Kubica, M. Kożuch, Testing procedures in evaluation of resistance of innovative shear connection with composite dowels, Arch. Civil Mech. Eng. 10 (3) (2010) 51–63.

[3] W. Lorenc, M. Kożuch, S. Rowiński, The behaviour of puzzle-shaped composite dowels. Pt. 1, Experimental study, J. Construct. Steel Res. 101 (2014) 482–499.

[4] W. Lorenc, M. Kożuch, S. Rowiński, The behaviour of puzzle-shaped composite dowels. Pt. 2, Theoretical investigations, J. Construct. Steel Res. 101 (2014) 500–518.

[5] G. Seidl, M. Stambuk, W. Lorenc, T. Kołakowski, E. Petzek, Wirtschaftliche Verbundbauweisen im Brückenbau – Bauweisen mit Verbunddübelleisten, Stahlbau 82 (Heft 7) (2013) 510–521.

[6] J. Berthellemy, W. Lorenc, M. Mensinger, S. Rauscher, G. Seidl, Zum Tragverhalten von Verbunddübeln, Teil 1: Tragverhalten unter statischer Belastung, Stahlbau 80 (Heft 3) (2011) 172–184.

[7] J. Berthellemy, W. Lorenc, M. Mensinger, J. Ndogmo, G. Seidl, Zum Tragverhalten von Verbunddübeln, Teil 2: Ermüdungsverhalten, Stahlbau 80 (Heft 4) (2011) 256–267.

[8] P. Harnatkiewicz, A. Kopczyński, M. Kożuch, W. Lorenc, S. Rowiński, Research on fatigue cracks in composite dowel shear connection, Eng. Fail. Anal. 18 (2011) 1279–1294.

[9] W. Dudziński, G. Pękalski, P. Harnatkiewicz, A. Kopczyński, W. Lorenc, M. Kożuch, S. Rowiński, Study on fatigue cracks in steel-concrete shear connection with composite dowels, Arch. Civil Mech. Eng. 11 (4) (2011) 839–858.

[10] E. Kubica, K. Rykaluk, W. Lorenc, M. Kożuch, Cutting of T-section from rolled beams in aspect of realisation composite girders (in polish). Zespolone konstrukcje mostowe, Kraków (2009).

[11] Bukała Grzegorz, Giergowicz Andrzej, Kołakowski Tomasz, Lorenc Wojciech, Przebudowa mostu kolejowego z zastosowaniem przęseł VFT-WIB®/Grzegorz Bukała [i in.], Eng. Construct. (4) (2011) 187–190.

[12] F. Möller, S. Möller, P. Collin, R. Hällmark, W. Lorenc, M. Kożuch, B. Norlin, O. Kero-koski, G. Seidl, T. Haariu, ELEM: Composite bridges with prefabricated decks, Draft, RFSR-CT-2008-00039, Final report. Project carried out with a financial grant from the Research Programme of the Research Fund for Coal and Steel.

[13] M. Kożuch, Resistance of MCL open steel connectors in steel concrete composite beams. Report PRE no. 3/2012 (PhD dissertation), Wrocław University of Technology, 2012.

[14] G. Seidl, Behaviour and load bearing capacity of composite dowels in steel-concrete composite girders. Report PRE no. 4/2009 (PhD dissertation), Wrocław University of Technology, 2009.

[15] W. Lorenc, Nośność ciągłych łączników otwartych w zespolonych konstrukcjach stalowo-betonowych (The design concept for the steel part of composite dowel shear

connection in steel-concrete composite structures). Wrocław, 2011.
[16] S. Rowiński, Fatigue strength of steel dowels in innovative shear connection of steel – concrete composite beam. Report PRE no. 4/2012 (PhD dissertation), Wrocław University of Technology, 2012.
[17] W. Lorenc, M. Kożuch, G. Seidl, Zur Grenztragfähigkeit von Verbunddübeln mit Klothoidenform, Stahlbau 82 (Heft 3) (2013) 196–207.
[18] ABAQUS Theory Manual, 2004.
[19] W. Lorenc, R. Ignatowicz, E. Kubica, G. Seidl, Numerical Model of Shear Connection by Concrete Dowels, Recent Developments in Structural Engineering Mechanics and Computation, Mill Press, Rotterdam, Netherlands, 2007.
[20] Allgemeine bauaufsichtliche Zulassung No. Z-26.4-56, Zulassungsgegenstand: Verbunddubelleisten, DIBt 2013.
[21] W. Lorenc, The design concept for the steel part of a composite dowel shear connection, Steel Construct. 9 (2) (2016) 89–97.